

Sensors & Diagnostics

rsc.li/sensors

The Royal Society of Chemistry is the world's leading chemistry community. Through our high impact journals and publications we connect the world with the chemical sciences and invest the profits back into the chemistry community.

IN THIS ISSUE

ISSN 2635-0998 CODEN SDEIAR 3(9) 1361-1580 (2024)



Cover

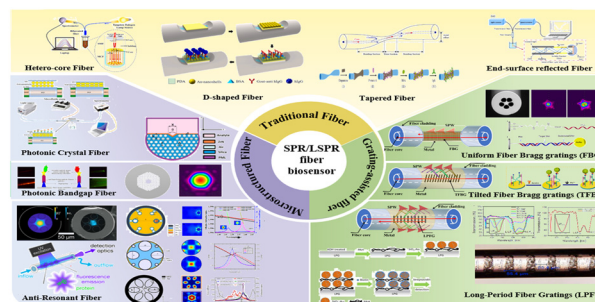
See Vagner Bezerra dos Santos, Carlos D. Garcia *et al.*, pp. 1467-1475.
Image reproduced by permission of Carlos D. Garcia from *Sens. Diagn.*, 2024, 3, 1467.

CRITICAL REVIEWS

1369

Recent advances of optical fiber biosensors based on surface plasmon resonance: sensing principles, structures, and prospects

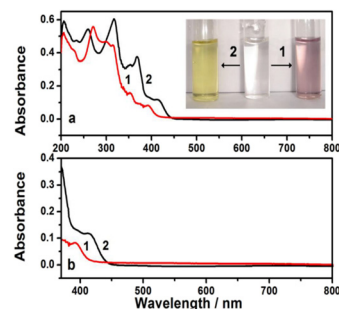
Jingwei Lv, Jianxin Wang, Lin Yang, Wei Liu, Haihao Fu, Paul K. Chu and Chao Liu*



1392

Optimization of solvents, electrolytes, and mediators for polyindole-based electrochemical sensors

P. C. Pandey,* Atul Kumar Tiwari and Roger J. Narayan*



ChemComm

Uncover new possibilities with outstanding preliminary research

Original discoveries, fuelling
every step of scientific progress

rsc.li/chemcomm

**Fundamental questions
Elemental answers**

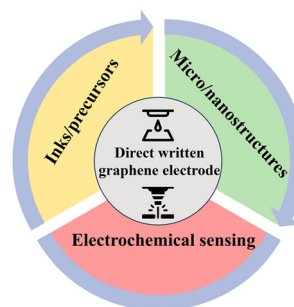


CRITICAL REVIEWS

1406

Direct writing of graphene electrodes for point-of-care electrochemical sensing applications

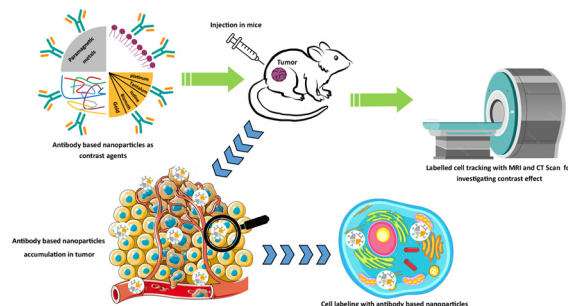
Lei Zhao,* Andrew Piper,* Giulio Rosati* and Arben Merkoçi*



1428

Antibody conjugates as CT/MRI Theranostics for diagnosis of cancers: a review of recent trends and advances

Saba Abaei, Ali Tarighatnia, Asghar Mesbahi and Ayuob Aghanejad*

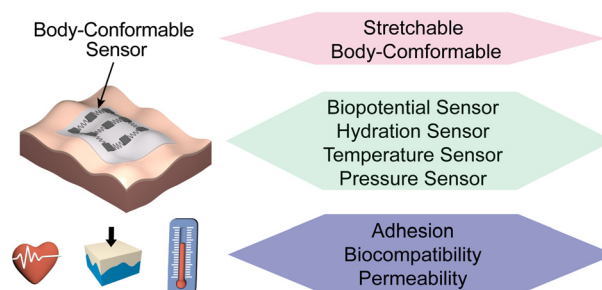


PERSPECTIVE

1442

Stretchable and body-conformable physical sensors for emerging wearable technology

Yong Lin, Weijie Qiu and Desheng Kong*

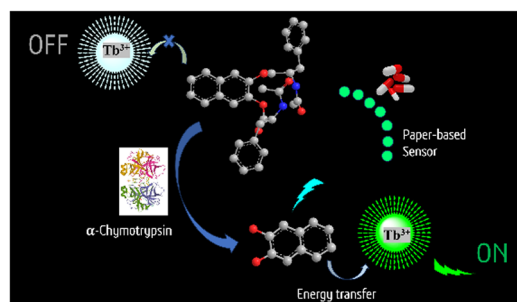


COMMUNICATIONS

1456

Paper-based sensing of pancreatic-cancer biomarker α -chymotrypsin through turn-on lanthanide-luminescence

Ananya Biswas and Uday Maitra*



The diagram illustrates the experimental setup for measuring the lipid bilayer capacitance. It shows a microfluidic device with an 'IN' inlet and a 'GND' (ground) connection. A dashed line indicates a magnified view of the lipid bilayer structure, showing 'Lipid-oil' and 'Lipid bilayer' components. The device is shown with a 75 mm scale bar.

Ji Huang, Yuval Elani and Mark S. Friddin*

Vagner Bezerra dos Santos,* Lucas B. Ayres,
Helayne Santos de Sousa, Carlos D. Garcia*
and Willian Toito Suarez

Figure 1 illustrates the synthesis and surface modification of La QDs. The top part shows the synthesis of La QDs from LaCl₃ and NaOH, resulting in a cluster of blue spheres. The bottom part shows the surface modification of La QDs with either a star-shaped shell (S) or a core-shell structure (H₂O₂) to form 'Turn On' fluorescent particles. A graph on the right shows the fluorescence intensity (a.u.) versus particle size (nm), with a sharp peak at 375 nm.

Amit Sahoo and Achyuta N. Acharya*

The diagram illustrates the iterative screening and optimization of a Ca^{2+} biosensor. The cycle includes the following steps:

- Screening:** A Hitachi microscope is used to screen a library of mutants.
- Top mutant:** The best-performing mutant is selected.
- Mutagenesis:** The selected mutant is used to create a new library of mutants.
- Transfection:** The new library of mutants is transfected into cells.
- Screening:** The process returns to the screening step to evaluate the new library.

An inset shows the Ca^{2+} biosensor protein structure and a fluorescence spectrum graph. The graph plots Fluorescence (0 to 1) against Wavelength (nm) (300 to 800). The spectrum shows a peak around 580 nm, with the $-\text{Ca}^{2+}$ condition (red line) showing higher fluorescence than the $+\text{Ca}^{2+}$ condition (black line).

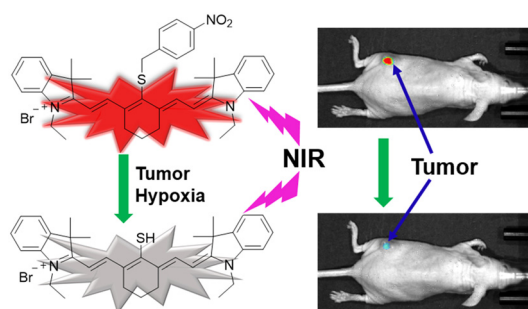
Yufeng Zhao,* Yi Shen, Teodor Veres
and Robert E. Campbell*

PAPERS

1505

A nitroreductase-sensitive near-IR fluorescent biosensor for detecting tumor hypoxia *in vivo*

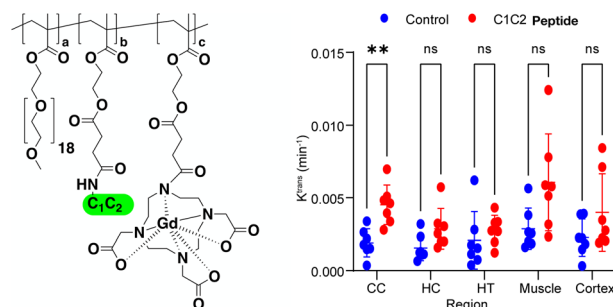
Safiya Nisar and Binglin Sui*



1513

Optimized gadolinium-DO3A loading in RAFT-polymerized copolymers for superior MR imaging of aging blood-brain barrier

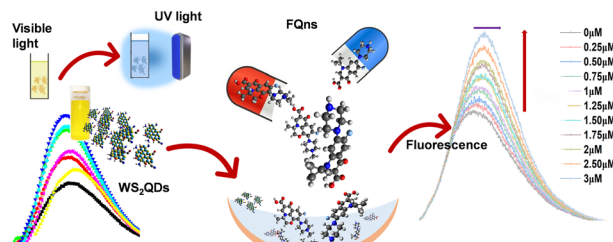
Hunter A. Miller, Aaron Priester, Evan T. Curtis, Krista Hilmas, Ashleigh Abbott, Forrest M. Kievit and Anthony J. Convertine*



1522

Highly efficient WS₂ QD-based non-enzymatic fluorescent biosensor for ofloxacin and ciprofloxacin monitoring in aquatic media

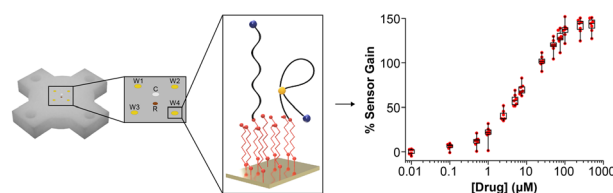
Sunayana Bora* and Chandan Upadhyay



1533

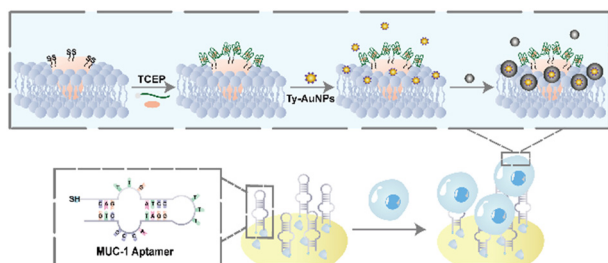
3D-printed electrochemical cells for multi-point aptamer-based drug measurements

John Mack, Raygan Murray, Kenedi Lynch and Netzahualcóyotl Arroyo-Currás*



PAPERS

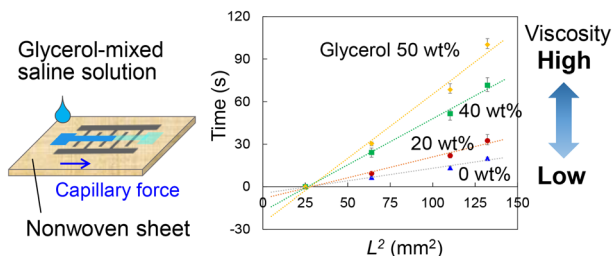
1542



Electrochemical detection of tumor cells based on proximity labelling-assisted multiple signal amplification

Guozhang Zhou, Fei Zhou, Xiaomeng Yu, Daiyuan Zhou, Jiaqi Wang, Bing Bo,* Ya Cao* and Jing Zhao*

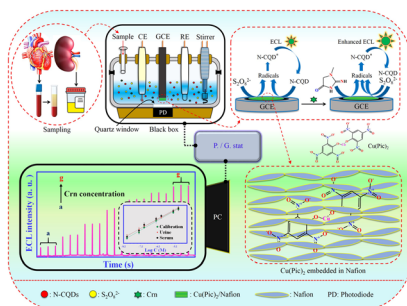
1551



Nonwoven-fabric-based microfluidic devices for solution viscosity measurements

Mayumi Otaba Uno,* Mariko Omori and Kenji Sakamoto

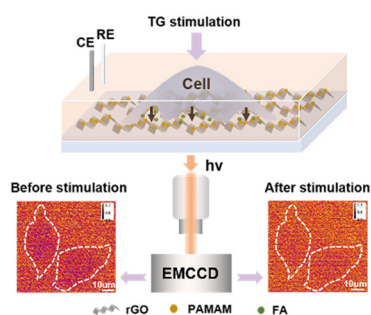
1562



A fast and highly selective ECL creatinine sensor for diagnosis of chronic kidney disease

Hosein Afshary and Mandana Amiri*

1571



In situ interface reaction-enabled electrochemiluminescence imaging for single-cell formaldehyde release analysis

Juanhua Zhou and Yang Liu*

